Eur Biophys J (2015) 44:437–446
DOI 10.1007/s00249-015-1044-7

ORIGINAL PAPER

EBSA
Biophysics in Europe

A novel and highly specific phage endolysin cell wall binding domain for detection of *Bacillus cereus*

Minsuk Kong[1] · Jieun Sim[2,3,4] · Taejoon Kang[2,3,4] · Hoang Hiep Nguyen[2,4] · Hyun Kyu Park[5] · Bong Hyun Chung[2,3,4] · Sangryeol Ryu[1]

Received: 13 March 2015 / Revised: 7 May 2015 / Accepted: 13 May 2015 / Published online: 5 June 2015

Abstract Rapid, specific and sensitive detection of pathogenic bacteria is crucial for public health and safety. *Bacillus cereus* is harmful as it causes foodborne illness and a number of systemic and local infections. We report a novel phage endolysin cell wall-binding domain (CBD) for *B. cereus* and the development of a highly specific and sensitive surface plasmon resonance (SPR)-based *B. cereus* detection method using the CBD. The newly discovered CBD from endolysin of PBC1, a *B. cereus*-specific bacteriophage, provides high specificity and binding capacity to *B. cereus*. By using the CBD-modified SPR chips, *B. cereus* can be detected at the range of 10^5–10^8 CFU/ml. More importantly, the detection limit can be improved to 10^2 CFU/ml by using a subtractive inhibition assay based on the pre-incubation of *B. cereus* and CBDs, removal of CBD-bound *B. cereus*, and SPR detection of the unbound CBDs. The present study suggests that the small and genetically engineered CBDs can be promising biological probes for *B. cereus*. We anticipate that the CBD-based SPR-sensing methods will be useful for the sensitive, selective, and rapid detection of *B. cereus*.

Keywords *Bacillus cereus* · Bacteriophage endolysin · Biosensor · Cell wall binding domain · Surface plasmon resonance

M. Kong and J. Sim contributed equally to this work.

Electronic supplementary material The online version of this article (doi:10.1007/s00249-015-1044-7) contains supplementary material, which is available to authorized users.

✉ Bong Hyun Chung
chungbh@kribb.re.kr

✉ Sangryeol Ryu
sangryu@snu.ac.kr

1 Department of Food and Animal Biotechnology, Department of Agricultural Biotechnology, Center for Food and Bioconvergence, Research Institute of Agriculture and Life Sciences, Seoul National University, Seoul 151-742, Korea

2 BioNanotechnology Research Center, KRIBB, Daejeon 305-806, Korea

3 BioNano Health Guard Research Center, KRIBB, Daejeon 305-806, Korea

4 Major of Nanobiotechnology, Korea University of Science and Technology, Daejeon 305-806, Korea

5 MicoBioMed Ltd, Daejeon 305-806, Korea

Introduction

Foodborne diseases are one of the most widespread and overwhelming public health problems of the modern world. In the USA, foodborne diseases cause an estimated 48 million illnesses each year, including 9.4 million episodes of illness, 55,961 hospitalizations, and 1351 deaths caused by known pathogens (Gould et al. 2013; Scallan et al. 2011). Additionally, outbreaks of foodborne illnesses result in economic losses totaling several billions of dollars annually (Abadian et al. 2014). Foodborne diseases can occur because of various kinds of bacteria, viruses, parasites, toxins, and so on. Among them, bacteria are the most common causes of foodborne diseases (Arora et al. 2011). For the identification of bacteria, conventional culture-based biochemical assays (Leoni and Legnani 2001) and DNA-based detection methods (Bej et al. 1991; Caliendo 2011; Lazcka et al. 2007; Mothershed and Whitney 2006; Olsen 2000) have been predominantly used. Additionally, several optical, electrical, electrochemical, and mechanical sensing approaches have been developed as alternatives (Abdel-Hamid et al. 1999; Baeumner et al. 2003; Brewster

et al. 1996; Croci et al. 2001; Radke and Alocilja 2005; Stephan et al. 2003; Taitt et al. 2004; Tims and Lim 2004; Vaughan et al. 2001; Velusamy et al. 2010; Wong et al. 2002). However, there are limitations with these methods such as the requirement of enrichment steps, long detection time, and need for labeling (Abdel-Hamid et al. 1999; Baeumner et al. 2003; Croci et al. 2001; Stephan et al. 2003; Taitt et al. 2004). Therefore, it is highly desired to develop simple, fast, sensitive, and accurate detection methods for pathogenic bacteria.

Antibodies are the most widely used biological probes for the detection of pathogenic bacteria (Singh et al. 2011). Production of specific antibodies, however, involves immunization of animals and maintenance of hybridoma cells, which are difficult, expensive, and time-consuming (Singh et al. 2012; Skottrup et al. 2008). Moreover, antibodies can lose their activity by changing temperature or pH and are prone to aggregation (Petrenko and Vodyanoy 2003; Wang et al. 2007). Accordingly, it is necessary to explore robust and specific biological probes. Bacteriophages, the natural enemy of bacteria, have been used as alternative probes for pathogenic bacteria sensing because they have extreme host specificity and strong resistance to heat, pH, and chemicals (Arya et al. 2011; Mahony et al. 2011; Tawil et al. 2014). Recently, bacteriophage-derived proteins have received more attention than whole bacteriophages since it is easy to modify the affinity and binding properties of these proteins (Brzozowska et al. 2015; Chibli et al. 2014; Javed et al. 2013; Poshtiban et al. 2013; Singh et al. 2011, 2010). Endolysin is a peptidoglycan hydrolase of bacteriophage that lyses its bacterial host at the end of the phage life cycle (Fischetti 2010; Loessner 2005). Endolysins from gram-positive bacteria-infecting phages consist of modular proteins including the C-terminal cell wall-binding domain (CBD) and N-terminal catalytic domain (Callewaert et al. 2011; Loessner et al. 2002). CBDs feature high specificity and strong binding affinity (K_D values of pico- to nanomolar range) to bacteria (Schmelcher et al. 2010, 2011). In addition, they are small (10–15 kDa), act as a monomer, and have no lytic activity. Furthermore, these superior features of CBDs can be improved by genetic engineering. Therefore, several recent studies have exploited CBDs as novel probes for the detection of bacteria (Kretzer et al. 2007; Tolba et al. 2012).

Herein, we report the highly sensitive and selective surface plasmon resonance (SPR)-based detection of *Bacillus cereus* by using a newly discovered phage endolysin CBD. SPR is a well-known technology that enables label-free, real-time, and quantitative detection of biomolecules, fulfilling the need for bacterial sensing (Abadian et al. 2014). *B. cereus* is harmful to humans because it causes foodborne illness (Bottone 2010); however, very few detection methods have been reported (Kang et al. 2013; Pal et al. 2007; Vaughan et al. 2003). Since the isolated CBD from endolysin of PBC1, a *B. cereus*-specific bacteriophage (Kong et al. 2012), exhibits high specificity and binding capacity to *B. cereus*, we could detect *B. cereus* at the range of 10^5–10^8 CFU/ml by using CBD-modified SPR chips. More importantly, *B. cereus* could be detected at the low concentration of 10^2 CFU/ml with a subtractive inhibition assay. This assay is based on the pre-incubation of *B. cereus* and CBDs, followed by removal of CBD-bound *B. cereus*, and SPR detection of the unbound CBDs. We anticipate that this novel CBD-based SPR sensing method will be useful for the sensitive, selective, and rapid detection of *B. cereus*.

Materials and methods

Bacteria culture conditions

B. cereus ATCC 21768, *Bacillus subtilis*, *Staphylococcus aureus*, *Salmonella typhi*, *Salmonella typhimurium*, *Salmonella enteritidis*, *Escherichia coli* O157:H7, *Listeria monocytogenes*, *Vibrio vulnificus*, *Yersinia enterocolitica*, and *Shigella sonnei* were used in this study. Bacteria were grown by streaking onto a Luria-Bertani (LB, Difco, Detroit, MI, USA) agar plate and incubated overnight at 37 °C. Next, a single colony from the agar plate was inoculated into 3 ml of LB media and incubated at 37 °C for 18 h with shaking at 200 rpm. One milliliter of bacterial culture was cultivated in a 250-ml flask with 100 ml of LB broth at 37 °C with shaking at 200 rpm. After 2 h, the optical density (OD) of the bacterial culture was measured at 600 nm by UV/Vis spectroscopy (Beckman Coulter, DU-800, Indianapolis, IN, USA). The read mode of spectroscopy was absorbance, and the average read time was 0.5 s. The CFU was calculated by the OD of the bacterial culture and the growth curve made by a plate count method. For SPR experiments, bacteria were centrifuged for 5 min at 16,000*g*, and the pellet was suspended in phosphate-buffered saline (PBS; 137 mM NaCl, 2.7 mM KCl, 8 mM Na_2HPO_4, and 2 mM KH_2PO_4; pH 7.4, Life Technologies, Seoul, Korea) after removing the supernatant. This step was performed in triplicate.

In silico analyses

Putative CBDs of LysPBC1 were identified through bioinformatic analyses. Amino acid sequence alignments of the reported CBDs were conducted using ClustalX2 (Larkin et al. 2007). A conserved domain search was conducted using BLASTP (Altschul et al. 1990), InterProScan (Zdobnov and Apweiler 2001), and NCBI Conserved Domain Database (Marchler-Bauer et al. 2007). Secondary and tertiary structures of PBC1 endolysin (LysPBC1) were

predicted using Phyre2 and the ESyPred3D server (Kelley and Sternberg 2009; Lambert et al. 2002). A gene fragment encoding 85 amino acids from the C-terminal of LysPBC1 was regarded as CBD, and the coding sequence was amplified by polymerase chain reaction (PCR) for subsequent steps. A phylogenetic tree of CBDs from reported *Bacillus* phage endolysins was generated with the MEGA5 program using the neighbor-joining method with *P*-distance values (Tamura et al. 2011).

Construction of recombinant proteins

The enhanced green fluorescent protein (EGFP) gene was amplified by PCR using pEGFP (Clontech, Palo Alto, CA, USA) as a template. The native stop codon was omitted for translational fusions. The amplified DNA product was double-digested using NdeI and BamHI and ligated into a pET28a vector (Novagen, Madison, WI, USA). The gene fragment encoding the CBD was digested with BamHI and HindIII and subcloned into the EGFP-containing pET28a. For SPR experiments, glutathione S-transferase (GST)-CBD fusion protein was employed. The GST coding gene was amplified by PCR using pGST parallel 1 as a template (Sheffield et al. 1999). A flexible linker region encoding six Gly and Ser residues was added between the GST and CBD genes to enable efficient protein folding. The sequences were verified for all constructs.

Expression and purification of CBD fusion proteins

N-Terminal six-His-tagged GFP-CBD fusion protein was produced in *E. coli* BL21 (DE3) (Invitrogen, Carlsbad, CA, USA). Freshly transformed cells were grown in LB at 37 °C to an OD_{600} of 0.7, and isopropyl-β-D-thiogalactoside (IPTG) (0.5 mM) was added. After incubation for 20 h at 18 °C, the cells were harvested by centrifugation, resuspended in a lysis buffer containing 200 mM NaCl and 50 mM Tris-Cl (pH 8.0) and frozen at −20 °C. After thawing, cells were lysed by sonication at a duty cycle of 25 % and output control of 5 (Sonifier 250, Branson, Danbury, CT, USA). After centrifugation (21,000*g*, 1 h, 4 °C) and sterilization by a 0.20-μm filter (Sartorious, Goettingen, Germany), the soluble protein was purified by immobilized metal affinity chromatography (Poly-Prep® chromatography column, catalog no. 731-1550, Bio-Rad, Hercules, CA, USA) using Ni-NTA agarose (Qiagen, Valencia, CA, USA). For affinity chromatography, the protein solution (5 ml) was incubated with 0.5 ml of the Ni-NTA resin for 1 h and followed by column purification by gravity flow. After washing the resin twice with the lysis buffer containing imidazole (10–20 mM), the protein was eluted in elution buffer (200 mM NaCl, 50 mM Tris-Cl, and 240 mM imidazole; pH 8.0) and divided into four 500-μl aliquots. The purity of the CBD fusion proteins was confirmed by sodium dodecyl sulfate-polyacrylamide gel electrophoresis (SDS-PAGE) with protein size marker (GenDEPOT, Barker, TX, USA). The purified protein was stored at −20 °C after buffer exchange to the storage buffer (50 mM Tris-Cl, 200 mM NaCl, and 50 % glycerol; pH 8.0) using PD Miditrap G-25 (GE Healthcare, Waukesha, WI, USA). The GST-CBD fusion protein was also produced by the same method as the GFP-CBD fusion protein. Before the SPR experiments, we exchanged the storage buffer into PBS by the PD-10 column (GE Healthcare, Seoul, Korea).

Cell-binding assay with fluorescence microscopy

The binding property of GFP-CBD fusion protein was examined as previously described (Loessner et al. 2002). Briefly, 1 ml of exponentially grown bacterial cells was centrifuged (16000*g*, 1 min) and resuspended in 1 ml of PBS. Next, 100 μl of cells was incubated together with 0.4 μM GFP-CBD fusion protein at room temperature for 5 min. The cells were washed twice with PBS buffer and observed by epifluorescence microscopy (DE/Axio Imager A1 microscope, Carl Zeiss, Oberkochen, Germany) with a GFP filter (470/40 nm excitation, 495 nm dichroic, 525/50 nm emission).

SPR analysis

The SPR instrument used in this study was the Biacore X (GE Healthcare, Pittsburgh, PA, USA). PBS was used as a running buffer. The baseline was established by flowing PBS for 300 s at the flow rate of 10 μl/min. For the preparation of the glutathione (GSH) chip, a bare Au chip (GE Healthcare, Pittsburgh, PA, USA) was cleaned by an N_2 stream and submerged in 1 mM GSH solution in dimethyl sulfoxide (DMSO). The GSH-attached Au chip was washed by DMSO and ethanol, then dried under an N_2 stream. Fifty microliters of 0.12 mg/ml GST-CBD in PBS was injected into the sample loop of the SPR instrument at a flow rate of 10 μl/min in order to attach the GST-CBD onto the GSH chip. PBS was continuously injected to remove the unbound GST-CBD. Finally, 50 μl of 1 mg/ml bovine serum albumin (BSA; reagent grade, Fisher, USA) in PBS was applied to prevent the non-specific binding. For the detection of bacteria, 50 μl of sample was injected across the chip surface at a flow rate of 10 μl/min, and the chip was washed in PBS.

To compare the binding capacity of the commercial antibody and CBD, the same molar concentration (3.2 μM) of anti-*Bacillus cereus* antibody (ab20556, Abcam, Seoul, Korea) and GST-CBD were used. For the immobilization of antibody molecules on the SPR chip, 50 μl of 0.1 mg/ml protein G (Bioprogen, Daejeon, Korea) was first applied

to a bare Au chip at a flow rate of 10 μl/min. Recombinant protein G is a widely used antibody-binding protein that has specific interactions with the Fc region of immunoglobulin G (Lee et al. 2007). After injection of protein G, 50 μl of 3.2 μM anti-*Bacillus cereus* antibody was applied to the SPR chip, and PBS was injected for 5 min to remove the unbound antibody. BSA in PBS was also injected across the chip to prevent the non-specific binding. The samples were finally injected.

In a subtractive inhibition assay, 500 μl of 5 μg/ml GST-CBD and *B. cereus* was mixed and incubated for 30 min at room temperature with occasional inverting. After incubation, the solution was centrifuged for 1-min intervals with a gradual speed increase (100, 120, 200, 450, 1000, and 1600*g*). Fifty microliters of supernatant was gathered and injected across the GSH chip at a flow rate of 10 μl/min. For the preparation of the *B. cereus*-contaminated food sample, 10 g of cooked rice was mixed with 90 ml of PBS and shaken on a shaker for 1 h. Then, 100 μl of *B. cereus* (10^8 CFU/ml) was added to 900 μl of the cooked rice sample. This *B. cereus*-inoculated sample was serially diluted ten-fold with the cooked rice sample to vary the concentration of *B. cereus*. For the detection of *B. cereus* in a food sample, 500 μl of 5 μg/ml GST-CBD and *B. cereus*-inoculated sample were mixed and incubated. After incubation, the solution was centrifuged, and 50 μl of supernatant was injected across the GSH chip.

Results and discussion

CBD from endolysin of *B. cereus* phage PBC1

PBC1 is a *B. cereus*-specific *Siphoviridae* phage with a 41,164-kb dsDNA genome (Kong et al. 2012). BLAST and domain searches showed that LysPBC1 consists of the N-acetylmuramoyl-L-alanine amidase with N-terminal Amidase_3 (PF01520) catalytic domain and the C-terminal Amidase02_C (PF12123) CBD (Fig. 1a). The N-terminal catalytic domain of LysPBC1 is significantly conserved with PlyPSA, while the putative CBD sequences of LysPBC1 and PlyPSA are totally different, suggesting that the putative CBD may determine host specificity. Phylogenetic analysis of the putative CBDs of the *B. cereus* group phages indicates that the CBD of LysPBC1 is unrelated to other CBDs except for the putative CBD of phage 12826 (Loessner et al. 1997) (Fig. 1b). The amino acid sequence identity between the CBD of LysPBC1 and the putative CBD of phage 12826 is 76 %. Because the putative CBD of phage 12826 has not been experimentally proven to date, we selected the CBD of LysPBC1 as a novel recognition element for *B. cereus*. Figure 1c shows a 3D model of LysPBC1 based on the structure of PlyPSA, an endolysin

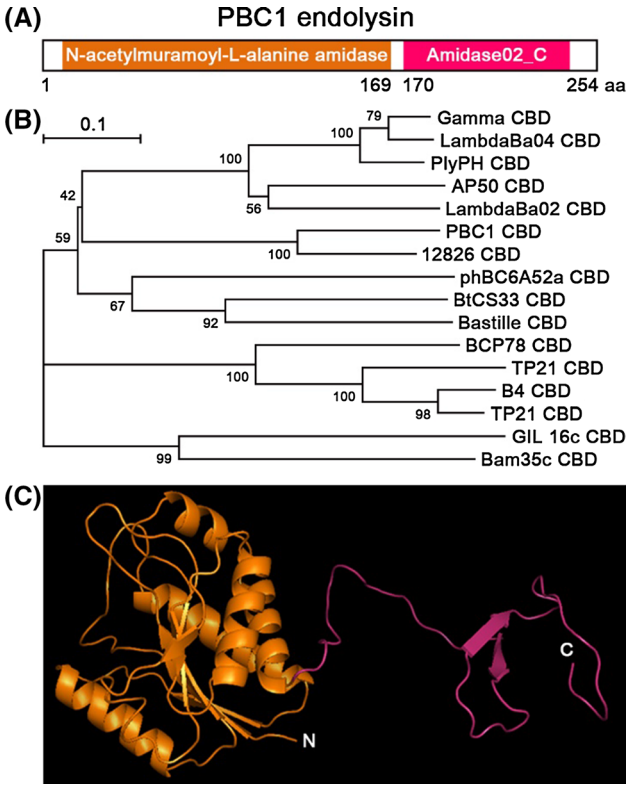

Fig. 1 **a** Schematic representation of PBC1 endolysin (LysPBC1). The N-terminal (*orange*) and C-terminal (*magenta*) domains are presented. **b** A phylogenetic tree indicating the relationships between CBDs examined in the present study. For calculation of the tree, the respective amino acid sequences, including the putative linker regions, were used. **c** Predicted 3D structure of LysPBC1 based on the crystal structure of *Listeria* phage endolysin PlyPSA (PDB 1D: 1XOV)

of *Listeria* phage PSA. This protein structure prediction enabled us to define the putative CBD region (magenta) in the endolysin sequence.

To examine the binding activity of CBD of LysPBC1, we genetically fused EGFP to the N-terminus of the CBD (Fig. 2a). The GFP-CBD fusion proteins were overexpressed in *E. coli* in the soluble form and easily purified by Ni-NTA affinity chromatography because of the N-terminal hexahistidine tag of the fusion proteins (Fig. 2b, c). The purified GFP-CBDs were added to intact *B. cereus* strain ATCC 21,768 cells, and the optical and fluorescent images were observed (Fig. 2d). The images clearly show that GFP-CBDs were uniformly attached to *B. cereus* cell surfaces. For comparison, only GFP was added to *B. cereus.* Figure 2e shows the optical and fluorescent images of *B. cereus* after the addition of GFP, indicating negligible binding of GFP to *B. cereus*. We further examined the binding specificity of the GFP-CBDs by mixing them with various bacterial species. None of the other bacterial species except *B. cereus* were labeled with GFP-CBDs, confirming that

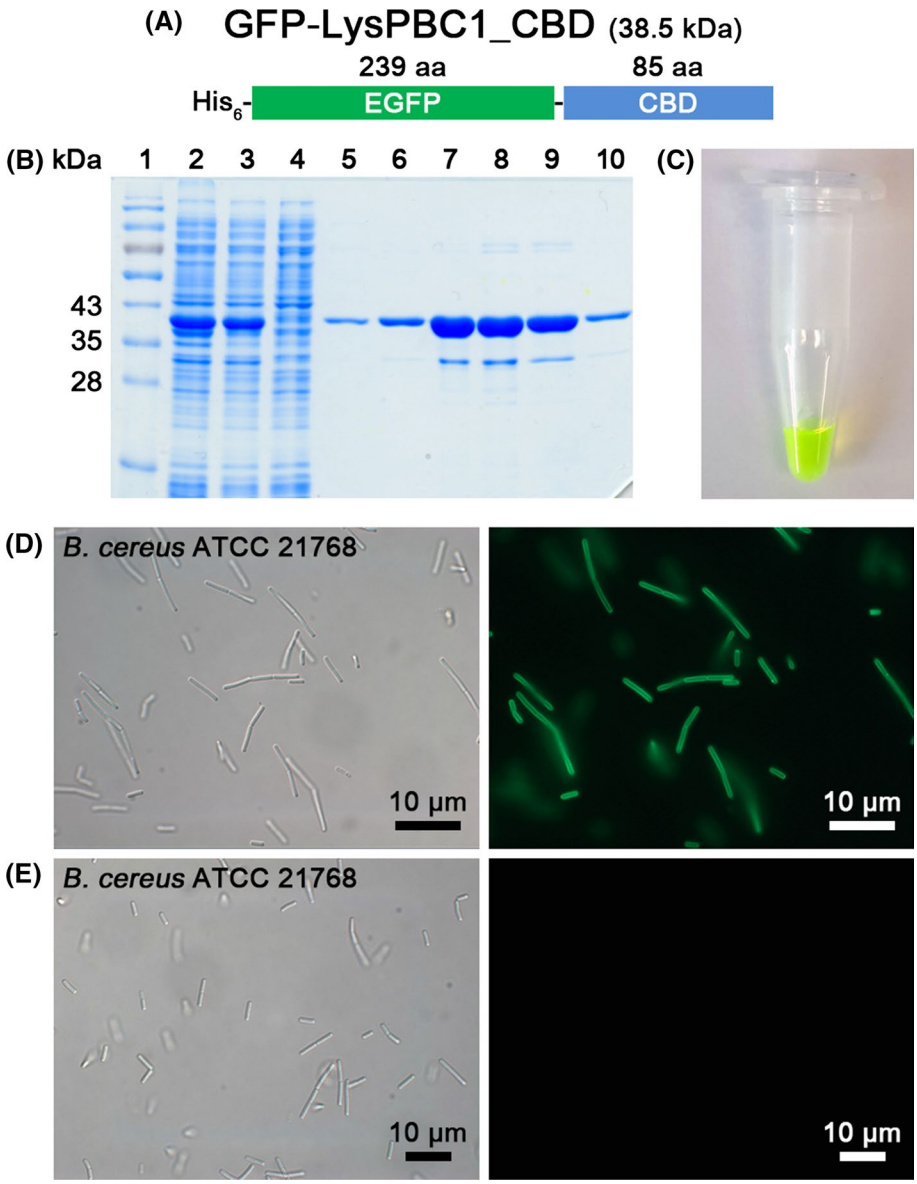

Fig. 2 **a** Schematic representation of GFP-LysPBC1_CBD. **b** SDS-PAGE analysis of GFP-CBD [*lane 1* size marker, *lane 2* cell extract, *lane 3* supernatant, *lane 4* Ni-NTA flow-through, *lane 5* washing (10 mM imidazole), *lane 6* washing (20 mM imidazole), *lane 7–10* elution (240 mM imidazole)]. **c** Image of the purified GFP-LysPBC1_CBD. **d**,**e** Optical and fluorescent images of *B. cereus* after the addition of GFP-LysPBC1_CBD and GFP. The fluorescent images show that *B. cereus* cell surfaces were evenly decorated with GFP-LysPBC1_CBD while GFP alone was not

the binding of GFP-CBDs was highly specific to *B. cereus* (Table 1 and Fig. S1). This result demonstrates that the CBDs of LysPBC1 can be highly specific biological probes for *B. cereus* detection.

SPR detection of *B. cereus* using CBDs

For SPR-based bacterial sensing, the use of CBDs is advantageous because the oriented immobilization of CBDs onto SPR chips can lead to the increased bacterial capture efficiency (Turkova 1999), whereas most antibodies are immobilized randomly onto SPR chips via reactive free amine coupling. To immobilize the CBDs onto a GSH chip, we genetically engineered the CBDs by adding GST genes to the N-terminal of CBDs (Fig. 3a). Since GST can bind to GSH with reasonable affinity and specificity (Chen et al. 2009; Pan et al. 2011; Singh et al. 2011; Tessema et al. 2006), GST-CBDs could be immobilized on the GSH chip in an oriented manner. Furthermore, GST-tag has been known to increase the recombinant protein solubility and to stabilize the protein by protecting the intracellular protease cleavage (Terpe 2003; Zhou and Wagner 2010). The recombinant GST-CBD fusion proteins were expressed solubly in *E. coli*, and the N-terminal hexahistidine tag facilitated the purification of the fusion proteins (Fig. 3b). Figure 3c shows the schematic illustration of *B. cereus* detection by using a CBD-modified SPR chip. First, a bare Au chip was coated with a self-assembled monolayer (SAM) of GSH. Next, GST-CBDs and BSA were flowed onto the GSH chip. Finally, *B. cereus* was flowed onto the CBD-modified SPR chip, and the SPR response was measured. Figure 3d shows the SPR

Table 1 Binding spectrum of LysPBC1_CBD

Species	Strain number	LysPBC1_CBD
Bacillus cereus	ATCC 21768	+
Bacillus thuringiensis	ATCC 10792	–
Bacillus mycoides	ATCC 6462	–
Bacillus megaterium	JCM 2506	–
Bacillus subtilis	ATCC 23857	–
Bacillus pumilus	JCM 2508	–
Bacillus licheniformis	JCM 2505	–
Bacillus sphaericus	JCM 2502	–
Bacillus circulans	JCM 2504	–
Listeria monocytogenes	Scott A	–
Listeria innocua	ATCC 33090	–
Staphylococcus aureus	ATCC 29213	–
Enterococcus faecalis	ATCC 29212	–
Escherichia coli	MG1655	–
Salmonella Typhimurium	SL1344	–
Shigella flexineri	2a strain 2457T	–
Cronobacter sakazakii	ATCC 29544	–

response curves obtained from CBD-modified SPR chips with different bacterial species. The concentration of bacteria was 10^7 CFU/ml. In the presence of *B. cereus*, the SPR response was highly increased (blue curve in Fig. 3d). However, the SPR response was not increased in the presence of *S. aureus*, *L. monocytogenes*, *S. sonnei*, *E. coli*, *Y. enterocolitica*, and even *B. subtilis*, a member of the genus *Bacillus*. This SPR result corresponds well with the above fluorescence results, clearly confirming that CBDs of LysPBC1 can detect *B. cereus* specifically.

Figure 3e presents SPR response curves obtained from CBD- and antibody-modified SPR chips after the injection of *B. cereus* of 10^7 CFU/ml. For the oriented immobilization of antibodies, protein G was employed. The SPR response intensity from the CBD-modified chip was over twice as high as that from the antibody-modified chip, suggesting that CBD has a stronger binding capacity than the antibody. Figure 3f shows the SPR response curves measured from CBD-modified SPR chips by changing the concentrations of *B. cereus*. The SPR response intensity

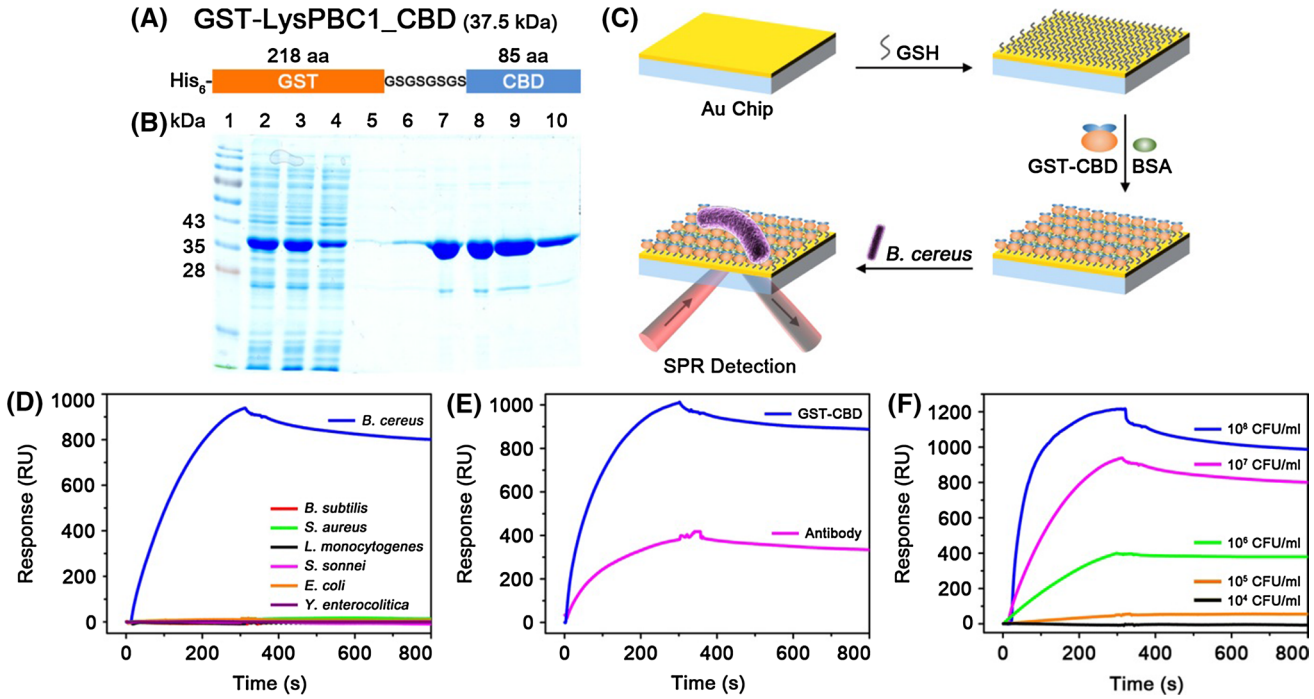

Fig. 3 **a** Schematic representation of GST-LysPBC1_CBD. **b** SDS-PAGE analysis of GST-CBD [*lane 1* size marker, *lane 2* cell extract, *lane 3* supernatant, *lane 4* Ni-NTA flow-through, *lane 5* washing (10 mM imidazole), *lane 6* washing (20 mM imidazole), *lane 7–10* elution (240 mM imidazole)]. **c** Schematic illustration of *B. cereus* detection using a CBD-modified SPR chip. First, a bare Au chip was coated with a SAM of GSH. Next, GST-LysPBC1_CBD and BSA were sequentially flowed onto the GSH chip. Finally, *B. cereus* was flowed onto the CBD-modified SPR chip, and the SPR response was measured. **d** SPR response curves obtained from CBD-modified SPR chips by varying bacterial species. The concentrations of bacteria were 10^7 CFU/ml. SPR response was highly increased in the presence of *B. cereus* (*blue curve*). **e** SPR response curves obtained from CBD- and antibody-modified SPR chips after the injection of *B. cereus*. The concentration of *B. cereus* was 10^7 CFU/ml. SPR response intensity from the CBD-modified chip was over two-fold higher than that from the antibody-modified chip, suggesting that CBD has a stronger binding capacity to *B. cereus* than antibody. **f** SPR response curves obtained from CBD-modified SPR chips by varying the concentrations of *B. cereus*. The SPR response intensities were reduced by decreasing the concentration from 10^8 to 10^5 CFU/ml

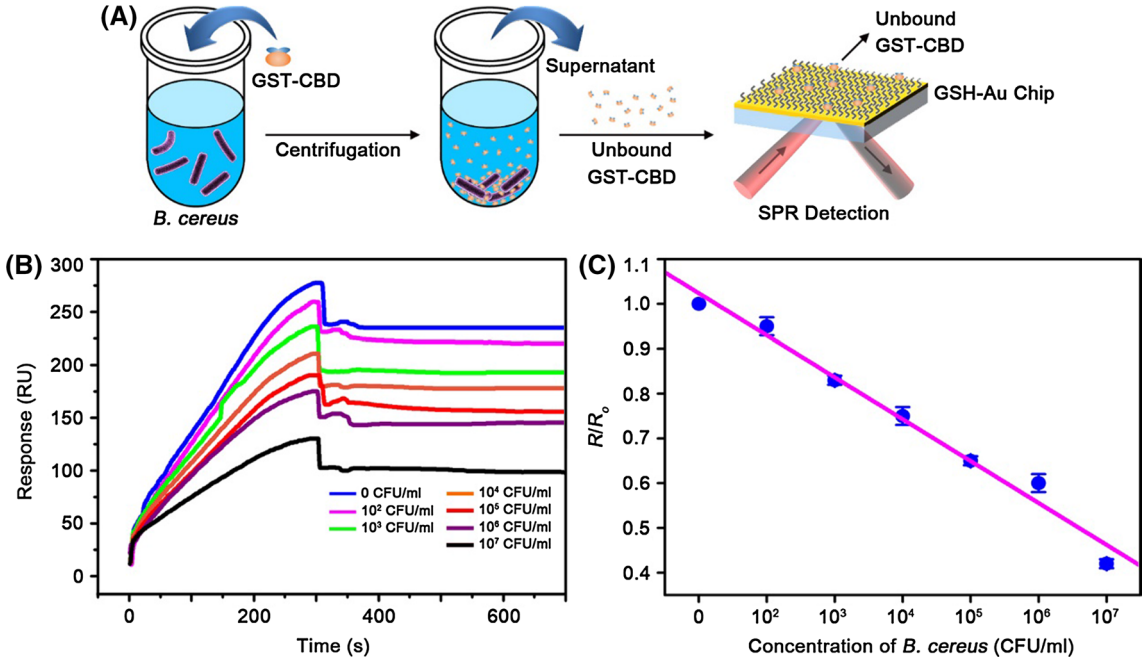

Fig. 4 **a** Schematic illustration of *B. cereus* detection using a subtractive inhibition assay. GST-CBD and *B. cereus* were incubated for 30 min, and unbound GST-CBD was separated from GST-CBD attached to *B. cereus* by centrifugation. Next, the supernatant was flowed onto a GSH chip, and the SPR response was measured. **b** SPR response curves obtained from GSH chips by varying the concentration of *B. cereus* in a subtractive inhibition assay. SPR response intensities decreased with increasing concentrations of *B. cereus* because the amount of unbound GST-CBD is inversely proportional to the concentration of *B. cereus*. By employing the subtractive inhibition assay, *B. cereus* could be detected at a concentration as low as 10^2 CFU/ml. **c** Plot of R/R_0 versus the concentration of *B. cereus*. R is a mean SPR response intensity at each concentration of *B. cereus*. R_0 is a mean SPR response intensity in the absence of *B. cereus*. A *magenta linear fit line* shows the dynamic range of 10^2–10^7 CFU/ml. Data represent the mean plus standard deviation from three measurements

decreased as the concentration of *B. cereus* was reduced from 10^8 to 10^5 CFU/ml. At 10^4 CFU/ml, the SPR response was indistinguishable. Therefore, the detection limit of this method was estimated to be 10^5 CFU/ml.

Improving *B. cereus* detection sensitivity by subtractive inhibition assay

In SPR sensing, the penetration depth of the evanescent field arising under conditions of total internal reflection cannot exceed 300 nm (Skottrup et al. 2008). Since most bacteria are larger than 300 nm, direct capture of bacteria can prevent effective penetration of the evanescent field, and thus SPR-based bacterial detection methods have limited sensitivity (Leonard et al. 2004). In order to improve the sensitivity of the SPR-based *B. cereus* detection method, we adopted a subtractive inhibition assay. Figure 4a shows a schematic illustration of *B. cereus* detection using a subtractive inhibition assay. GST-CBDs and *B. cereus* were incubated for 30 min at room temperature with occasional inverting. After incubation, unbound GST-CBDs were separated from GST-CBD-attached *B. cereus* by sequential centrifugation. The centrifugation speed was increased gradually to distinguish the unbound GST-CBDs and the GST-CBD-attached *B. cereus*. We carefully gathered the supernatant containing the unbound GST-CBDs. The supernatant was flowed onto GSH chips, and the SPR response was measured. Figure 4b shows the SPR response curves obtained from GSH chips by varying the concentration of *B. cereus* in a subtractive inhibition assay. In the absence of *B. cereus*, the response intensity was highest. By increasing the concentration of *B. cereus*, the intensity decreased because the amount of unbound GST-CBDs was inversely proportional to the concentration of *B. cereus*. At a concentration as low as 10^2 CFU/ml, *B. cereus* could be detected by employing a subtractive inhibition assay. Figure 4c is the plot of R/R_0 versus concentration of *B. cereus*. R is the mean SPR response intensity at each concentration of *B. cereus*, and R_0 is the mean SPR response intensity in the absence of *B. cereus*. The plot verifies that the quantitative detection of *B. cereus* is possible at the range of 10^2–10^7 CFU/ml. Compared to the direct sensing result in Fig. 3f, the detection limit is improved three orders of magnitude.

Lastly, we tried to detect *B. cereus* in a food sample using subtractive inhibition assay. Cooked rice was used

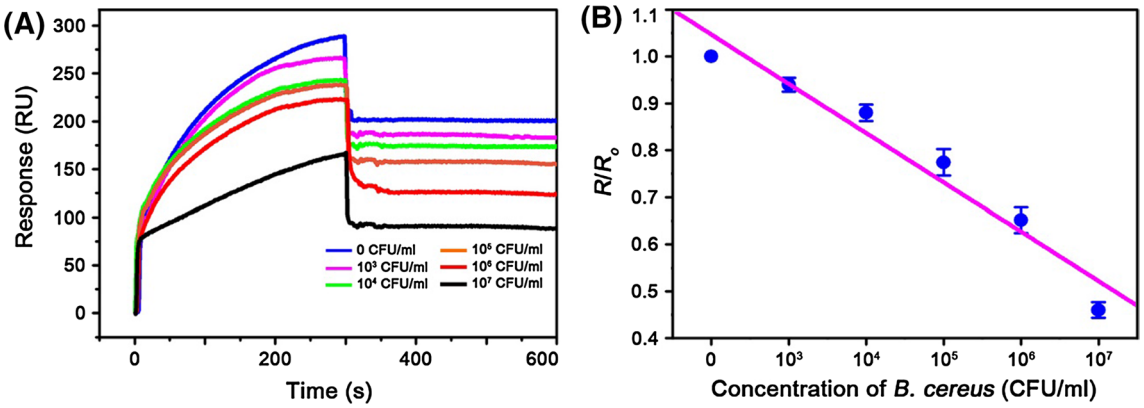

Fig. 5 Detection of *B. cereus* in a cooked rice sample by using a subtractive inhibition assay. **a** SPR response curves obtained from GSH chips by varying the concentration of *B. cereus* in a cooked rice sample. SPR response intensities decreased with increasing concentrations of *B. cereus*. In a cooked rice sample, *B. cereus* could be detected at a concentration as low as 10^3 CFU/ml. **b** Plot of R/R_0 versus the concentration of *B. cereus*. *R* is a mean SPR response intensity at each concentration of *B. cereus*. R_0 is a mean SPR response intensity in the absence of *B. cereus*. A *magenta linear fit line* shows the dynamic range of 10^3–10^7 CFU/ml. Data represent the mean plus standard deviation from three measurements

as a food matrix because it is the food most commonly polluted by *B. cereus* (Rangan 2008). Figure 5a shows the SPR response curves obtained from GSH chips by varying the concentration of *B. cereus* in a cooked rice sample. One thousand (10^3) CFU/ml of *B. cereus* could be detected in a cooked rice sample. Plot of R/R_0 versus the concentration of *B. cereus* in a cooked rice sample shows that the quantitative detection of *B. cereus* is possible at the range of 10^3–10^7 CFU/ml (Fig. 5b). Compared with the results of pure *B. cereus* detection, the sensitivity was depressed. This may be attributed to the non-specific adsorption of carbohydrates, proteins, etc. The successful detection of *B. cereus* in a cooked rice sample demonstrates the feasibility of the CBD-based SPR sensing method for the detection of *B. cereus* in complex food samples.

B. cereus causes not only foodborne illness, but also a number of systemic and local infections, yet very few detection methods employing mechanical, electrical, or electrochemical sensors have been developed (Kang et al. 2013; Pal et al. 2007; Vaughan et al. 2003). This is the first report of SPR-based *B. cereus* sensing, which enables sensitive, specific, and convenient detection of *B. cereus*.

Conclusion

We report a novel phage endolysin CBD for *B. cereus* and development of a highly specific and sensitive SPR-based *B. cereus* detection method using the CBD. The present study has the following important features. First, the newly discovered CBD is very specific to *B. cereus* and exhibits a higher binding capacity than a commercial antibody. Therefore, the CBD can be used as an excellent biological probe for the detection of *B. cereus*. Second, to the best of our knowledge, this is the first report of SPR-based *B. cereus* detection. We detected 10^5 CFU/ml of *B. cereus* by CBD-modified SPR chips, and the detection limit could be lowered to 10^2 CFU/ml using a subtractive inhibition assay. Third, *B. cereus* in a food sample could be detected at the low concentration of 10^3 CFU/ml. We anticipate that this result will advance us a step closer to rapid, sensitive, and selective detection of *B. cereus*.

Acknowledgments This research was supported by the Public Welfare & Safety research program (NRF-2012M3A2A1051684, NRF-2012M3A2A1051682) through the National Research Foundation of Korea funded by the Ministry of Science, ICT and Future Planning (MSIP), Global Frontier Project (H-GUARD_2013M3A6B2078950, H-GUARD_2014M3A6B2060489) through the Center for Bio-Nano Health-Guard funded by the MSIP, and KRIBB initiative Research Program.

References

Abadian PN, Kelley CP, Goluch ED (2014) Cellular analysis and detection using surface plasmon resonance techniques. Anal Chem 86:2799–2812

Abdel-Hamid I, Ivnitski D, Atanasov P, Wilkins E (1999) Flow-through immunofiltration assay system for rapid detection of *E. coli* O157:H7. Biosens Bioelectron 14:309–316

Altschul SF, Gish W, Miller W, Myers EW, Lipman DJ (1990) Basic local alignment search tool. J Mol Biol 215:403–410

Arora P, Sindhu A, Dilbaghi N, Chaudhury A (2011) Biosensors as innovative tools for the detection of food borne pathogens. Biosens Bioelectron 28:1–12

Arya SK, Singh A, Naidoo R, Wu P, McDermott MT, Evoy S (2011) Chemically immobilized T4-bacteriophage for specific *Escherichia coli* detection using surface plasmon resonance. Analyst 136:486–492

Baeumner AJ, Cohen RN, Miksic V, Min J (2003) RNA biosensor for the rapid detection of viable Escherichia coli in drinking water. Biosens Bioelectron 18:405–413

Bej AK, Mahbubani MH, Dicesare JL, Atlas RM (1991) Polymerase chain reaction-gene probe detection of microorganisms by using filter-concentrated samples. Appl Environ Microbiol 57:3529–3534

Bottone EJ (2010) *Bacillus cereus*, a volatile human pathogen. Clin Microbiol Rev 23:382–398

Brewster JD, Gehring AG, Mazenko RS, Houten LJV, Crawford CJ (1996) Immunoelectrochemical assays for bacteria: use of epifluorescence microscopy and rapid-scan electrochemical techniques in development of an assay for *Salmonella*. Anal Chem 68:4153–4159

Brzozowska E, Smietana M, Koba M, Gorska S, Pawlik K, Gamian A, Bock WJ (2015) Recognition of bacterial lipopolysaccharide using bacteriophage-adhesin-coated long-period gratings. Biosens Bioelectron 67:93–99

Caliendo AM (2011) Multiplex PCR and emerging technologies for the detection of respiratory pathogens. Clin Infect Dis 52(Suppl 4):S326–S330

Callewaert L, Walmagh M, Michiels CW, Lavigne R (2011) Food applications of bacterial cell wall hydrolases. Curr Opin Biotech 22:164–171

Chen LH, Wang Q, Hou WG (2009) The utilization of BSA-modified chip on the investigation of ligand/protein interaction with surface plasma resonance. Afr J Biotechnol 8:7148–7155

Chibli H, Ghali H, Park S, Peter YA, Nadeau JL (2014) Immobilized phage proteins for specific detection of staphylococci. Analyst 139:179–186

Croci L, Delibato E, Volpe G, Palleschi G (2001) A rapid electrochemical ELISA for the detection of *Salmonella* in meat samples. Anal Lett 34:597–2607

Fischetti VA (2010) Bacteriophage endolysins: a novel anti-infective to control Gram-positive pathogens. Int J Med Microbiol 300:57–362

Gould LH, Walsh KA, Vieira AR, Herman K, Williams IT, Hall AJ, Cole D (2013) Surveillance for foodborne disease outbreaks—United States, 1998–2008. MMWR Surveill Summ 62:1–34

Javed MA, Poshtiban S, Arutyunov D, Evoy S, Szymanski CM (2013) Bacteriophage receptor binding protein based assays for the simultaneous detection of *Campylobacter jejuni* and *Campylobacter coli*. PLoS One 8:e69770. doi:10.1371/journal.pone.0069770

Kang XB, Pang GC, Chen QS, Liang XY (2013) Fabrication of *Bacillus cereus* electrochemical immunosensor based on double-layer gold nanoparticles and chitosan. Sens Actuat B-Chem 177:1010–1016

Kelley LA, Sternberg MJ (2009) Protein structure prediction on the Web: a case study using the Phyre server. Nat Protoc 4:63–371

Kong M, Kim M, Ryu S (2012) Complete genome sequence of *Bacillus cereus* bacteriophage PBC1. J Virol 86:6379–6380

Kretzer JW, Lehmann R, Schmelcher M, Banz M, Kim KP, Korn C, Loessner MJ (2007) Use of high-affinity cell wall-binding domains of bacteriophage endolysins for immobilization and separation of bacterial cells. Appl Environ Microb 73:992–2000

Lambert C, Leonard N, De Bolle X, Depiereux E (2002) ESyPred3D: prediction of proteins 3D structures. Bioinformatics 18:1250–1256

Larkin MA, Blackshields G, Brown NP, Chenna R, McGettigan PA, McWilliam H, Valentin F, Wallace IM, Wilm A, Lopez R, Thompson JD, Gibson TJ, Higgins DG (2007) Clustal W and Clustal X version 2.0. Bioinformatics 23:2947–2948

Lazcka O, Del Campo FJ, Munoz FX (2007) Pathogen detection: a perspective of traditional methods and biosensors. Biosens Bioelectron 22:1205–1217

Lee JM, Park HK, Jung Y, Kim JK, Jung SO, Chung BH (2007) Direct immobilization of protein G variants with various numbers of cysteine residues on a gold surface. Anal Chem 79:2680–2687

Leonard P, Hearty S, Quinn J, O'Kennedy R (2004) A generic approach for the detection of whole *Listeria monocytogenes* cells in contaminated samples using surface plasmon resonance. Biosens Bioelectron 19:1331–1335

Leoni E, Legnani PP (2001) Comparison of selective procedures for isolation and enumeration of *Legionella* species from hot water systems. J Appl Microbiol 90:27–33

Loessner MJ (2005) Bacteriophage endolysins—current state of research and applications. Curr Opin Microbiol 8:480–487

Loessner MJ, Maier SK, Daubek-Puza H, Wendlinger G, Scherer S (1997) Three *Bacillus cereus* bacteriophage endolysins are unrelated but reveal high homology to cell wall hydrolases from different bacilli. J Bacteriol 179:2845–2851

Loessner MJ, Kramer K, Ebel F, Scherer S (2002) C-terminal domains of *Listeria monocytogenes* bacteriophage murein hydrolases determine specific recognition and high-affinity binding to bacterial cell wall carbohydrates. Mol Microbiol 44:335–349

Mahony J, McAuliffe O, Ross RP, van Sinderen D (2011) Bacteriophages as biocontrol agents of food pathogens. Curr Opin Biotech 22:157–163

Marchler-Bauer A, Anderson JB, Derbyshire MK, DeWeese-Scott C, Gonzales NR, Gwadz M, Hao L, He S, Hurwitz DI, Jackson JD, Ke Z, Krylov D, Lanczycki CJ, Liebert CA, Liu C, Lu F, Lu S, Marchler GH, Mullokandov M, Song JS, Thanki N, Yamashita RA, Yin JJ, Zhang D, Bryant SH (2007) CDD: a conserved domain database for interactive domain family analysis. Nucl Acids Res 35:D237–D240

Mothershed EA, Whitney AM (2006) Nucleic acid-based methods for the detection of bacterial pathogens: present and future considerations for the clinical laboratory. Clin Chim Acta 363:206–220

Olsen JE (2000) DNA-based methods for detection of food-borne bacterial pathogens. Food Res Int 33:257–266

Pal S, Alocilja EC, Downes FP (2007) Nanowire labeled direct-charge transfer biosensor for detecting *Bacillus* species. Biosens Bioelectron 22:2329–2336

Pan Y, Long MJC, Li XM, Shi Jf, Hedstrom L, Xu B (2011) Glutathione (GSH)-decorated magnetic nanoparticles for binding glutathione-S-transferase (GST) fusion protein and manipulating live cells. Chem Sci 2:945–948

Petrenko VA, Vodyanoy VJ (2003) Phage display for detection of biological threat agents. J Microbiol Meth 53:253–262

Poshtiban S, Javed MA, Arutyunov D, Singh A, Banting G, Szymanski CM, Evoy S (2013) Phage receptor binding protein-based magnetic enrichment method as an aid for real time PCR detection of foodborne bacteria. Analyst 138:5619–5626

Radke SM, Alocilja EC (2005) A high density microelectrode array biosensor for detection of *E. coli* O157:H7. Biosens Bioelectron 20:1662–1667

Rangan C (2008) *Bacillus cereus*. In: Barceloux DG (ed) Medical toxicology of natural substances: foods, fungi, medicinal herbs, plants, and venomous animals. Wiley, New Jersey, pp 89–95

Scallan E, Hoekstra RM, Angulo FJ, Tauxe RV, Widdowson MA, Roy SL, Jones JL, Griffin PM (2011) Foodborne illness acquired in the United States—major pathogens. Emerg Infect Dis 17:7–15

Schmelcher M, Shabarova T, Eugster MR, Eichenseher F, Tchang VS, Banz M, Loessner MJ (2010) Rapid multiplex detection and differentiation of *Listeria* cells by use of fluorescent phage endolysin cell wall binding domains. Appl Environ Microb 76:5745–5756

Schmelcher M, Tchang VS, Loessner MJ (2011) Domain shuffling and module engineering of *Listeria* phage endolysins for enhanced lytic activity and binding affinity. Microb Biotechnol 4:651–662

Sheffield P, Garrard S, Derewenda Z (1999) Overcoming expression and purification problems of RhoGDI using a family of "parallel" expression vectors. Protein Expr Purif 15:34–39

Singh A, Arya SK, Glass N, Hanifi-Moghaddam P, Naidoo R, Szymanski CM, Tanha J, Evoy S (2010) Bacteriophage tailspike proteins as molecular probes for sensitive and selective bacterial detection. Biosens Bioelectron 26:131–138

Singh A, Arutyunov D, McDermott MT, Szymanski CM, Evoy S (2011) Specific detection of *Campylobacter jejuni* using the bacteriophage NCTC 12673 receptor binding protein as a probe. Analyst 136:4780–4786

Singh A, Arutyunov D, Szymanski CM, Evoy S (2012) Bacteriophage based probes for pathogen detection. Analyst 137:3405–3421

Skottrup PD, Nicolaisen M, Justesen AF (2008) Towards on-site pathogen detection using antibody-based sensors. Biosens Bioelectron 24:339–348

Stephan R, Schumacher S, Zychowska MA (2003) The VIT® technology for rapid detection of *Listeria monocytogenes* and other *Listeria* spp. Int J Food Microbiol 89:287–290

Taitt CR, Golden JP, Shubin YS, Shriver-Lake LC, Sapsford KE, Rasooly A, Ligler FS (2004) A portable array biosensor for detecting multiple analytes in complex samples. Microb Ecol 47:175–185

Tamura K, Peterson D, Peterson N, Stecher G, Nei M, Kumar S (2011) MEGA5: molecular evolutionary genetics analysis using maximum likelihood, evolutionary distance, and maximum parsimony methods. Mol Biol Evol 28:2731–2739

Tawil N, Sacher E, Mandeville R, Meunier M (2014) Bacteriophages: biosensing tools for multi-drug resistant pathogens. Analyst 139:1224–1236

Terpe K (2003) Overview of tag protein fusions: from molecular and biochemical fundamentals to commercial systems. Appl Microbiol Biotechnol 60:523–533

Tessema M, Simons PC, Cimino DF, Sanchez L, Waller A, Posner RG, Wandinger-Ness A, Prossnitz ER, Sklar LA (2006) Glutathione-S-transferase-green fluorescent protein fusion protein reveals slow dissociation from high site densiy beads and measures free GSH. Cytom Part A 69A:326–334

Tims TB, Lim DV (2004) Rapid detection of *Bacillus anthracis* spores directly from powders with an evanescent wave fiber-optic biosensor. J Microbiol Meth 59:127–130

Tolba M, Ahmed MU, Tlili C, Eichenseher F, Loessner MJ, Zourob M (2012) A bacteriophage endolysin-based electrochemical impedance biosensor for the rapid detection of *Listeria* cells. Analyst 137:5749–5756

Turkova J (1999) Oriented immobilization of biologically active proteins as a tool for revealing protein interactions and function. J Chromatogr B 722:11–31

Vaughan RD, O'Sullivan CK, Guilbault GG (2001) Development of a quartz crystal microbalance (QCM) immunosensor for the detection of *Listeria monocytogenes*. Enzym Microb Tech 29:635–638

Vaughan RD, Carter RM, O'Sullivan CK, Guilbault GG (2003) A quartz crystal microbalance (QCM) sensor for the detection of *Bacillus cereus*. Anal Lett 36:731–747

Velusamy V, Arshak K, Korostynska O, Oliwa K, Adley C (2010) An overview of foodborne pathogen detection: in the perspective of biosensors. Biotechnol Adv 28:232–254

Wang W, Singh S, Zeng DL, King K, Nema S (2007) Antibody structure, instability, and formulation. J Pharm Sci-Us 96:1–26

Wong YY, Ng SP, Ng MH, Si SH, Yao SZ, Fung YS (2002) Immunosensor for the differentiation and detection of *Salmonella* species based on a quartz crystal microbalance. Biosens Bioelectron 17:676–684

Zdobnov EM, Apweiler R (2001) InterProScan—an integration platform for the signature-recognition methods in InterPro. Bioinformatics 17:847–848

Zhou P, Wagner G (2010) Overcoming the solubility limit with solubility-enhancement tags: successful applications in biomolecular NMR studies. J Biomol NMR 46:23–31